NASA GRANT NAG 5-1273
1989-1992

FINAL REPORT

Preamble:
The grant was awarded to investigate two areas that are related to planetary gamma-ray spectrometry. The first task wase the inestigation of gamma rays produced by high-enegy charged particles and their secondaries in planetary surfaces by means of thick target bombardments. The second task was the investigation of the effects of high-energy neutrons on gamma-ray spectral features obtained with high-purity Ge-detectors. For both tasks, as a function of the funding level, the experimental work was predominantly tied to that of other researchers, whenever there was an opportunity to participate in bombardment experiments at large or small accelerators for charged particles.

Report:

Task 1: Simulation experiments with 800 MeV, 1.5 and 2.5 GeV protons for the interpretation of lunar gamma-ray spectra.

During the report period we participated in four thick target bombardment experiments. Three of these experiments were performed at the Los Alamos Meson Physics Facility. One additional experiment was performed at the SATURNE accelerator at Saclay, France.

In all of these experiments one of the major components for the production of gamma-rays are secondary neutrons. In the Los Alamos experiments therefore the major task was to measure the secondary neutron distribution within thick targets exposed to 800 MeV neutrons. In the SATURNE 1.5 and 2.5 GeV experiment this approach was not possible, and therefore escaping neutrons and gamma-rays were measured.

The experiments revealed the spatial distribution of secondary neutrons throughout the volume of the thick targets exposed, and in the case of the Saturne irradiation, the relation between escaping neutrons and gamma-rays produced. These findings are directly appicable to the interpretation of gamma-ray spectra obtained from planetary surfaces.

The results of these experiments were presented at Lunar an Planetary Science Conferences and at one Meteoritical Society conference. A list of published abstracts is attached.

Task 2: Determination of energetic neutron fluxes via features of gamma-ray spectra:

Germanium detectors used in planetary gamma-ray spectrometry are exposed to neutrons escaping from the planetary surface. these neutrons carry information on the moderator content of the planetary surface and hence could be used to estimate water or carbondioxide abundances. The spectral features to be used are neutron scattering gamma-ray lines of germanium isotopes.

Interactions of neutrons with germanium detectors were investigated by exposing HPGe detectors into beams of neutrons with a well characterized energy spectrum and flux. Several exposures between 10MeV and 68MeV maximum neutron energy were done at the Cyclotron of the Crocker Nuclear Laboratory. It was discovered that the germanium inelastic scattering peaks of the gamma-ray spectr taken could be analyzed qualitatively with simple methods to reflect the neutron energy spectrum. Quantitative assesments of flux and senergy spectrum of neutrons, however needs to rely on more experimental work.

The results are compiled in a draft of a publication, which is attached to this report.

PUBLICATIONS

P.A.J. Englert, D.M. Drake, E.R. Shunk, M. Drosg, R.C. Reedy, J. Brückner, 1990. "Simulation of galactic cosmic ray interactions with 'martian soil': Implication for cosmogenic nuclide studies and planetary gamma ray spectroscopy". Lunar Planet. Sci. Conf. XXI, 325-326.

Peter A.J. Englert, Darrell M. Drake, Edward R. Shunk, Manfred Drosg, Robert C. Reedy, and Johannes Brueckner (1990), "Thick Target Bombardments: Cosmogenic Nuclide Production in Planetary Soil," Meteoritics 25, 361.

D.M. Drake, S.A. Wender, R.O. Nelson, D.D. Clark, M. Drosg, W. Armian, J. Brückner, P.A.J. Englert, 1991. "Experimental Simulation of Martian Neutron Leakage Spectra". Nucl. Instr. Meth. A309, 575-580.

S.G. Bobias, J. F. Dempsey, P.A.J. Englert, D.M. Drake, and R.C. Reedy (1992). Simulation of galactic cosmic ray interactions with regolith: Implications for cosmogenic nuclide and planetary surface studies. Meteoritics 27, 205.

J. Brückner, U. Fabian, A. Patnaik, H. Wänke, P. Cloth, G. Dagge, V. Drüke, D. Filges, P.A.J. Englert, D.M. Drake, R.C. Reedy, (1992). "Simulations Experiments for planetary gamma-ray spectroscopy by means of thick target high-energy proton irradiations." Lunar and Planetary Sci. Conf. XXIII, 169.

NEUTRON ENERGY DETERMINATION with A HIGH-PURITY GERMANIUM DETECTOR

FEBRUARY 20, 1992

GENE A. BECK

ABSTRACT

NEUTRON ENERGY DETERMINATION UTILIZING A HIGH-PURITY GERMANIUM DETECTOR

This article evaluates the use of germanium gamma-ray detectors to determine the energy of incident neutrons in the range of 10-70 MeV. Methods were developed to separate the nuclear recoil spectra from the gamma ray spectra produced in neutron inelastic scattering. The germanium 596, 690 and 835 kev (n,n'γ) peaks were evaluated for full width maximum values, and the slopes were determined for the leading edge and for the primary downslope.

Findings indicate that the full width maximum values were not useful indicators of neutron energies. This may be due to the "bleeding" of activity ie. background, from one recoil peak into the next recoil peak. Evaluation of the upslope and downslope measurements showed a relationship between the neutron energy and the values of these slopes for all three recoil peaks. A series of equations were developed to describe these relationships empirically. The germanium detector can now be used by Health Physicists to measure gamma ray spectra as well as to evaluate neutron sources for energy and exposure.

1. Introduction

Neutron dosimetry, particularly when applied to fast neutrons, depends strongly on the energy of the neutrons. [1,2] The current methods used for measuring exposure from neutrons are valid up to approximately 15 MeV. Present methods include the use of Hurst counters, rem meters, and albedo neutron dosimeters. [3] The principal problem that these instruments have at higher energy levels is their non-linear response to the neutron energy. There are many instances where the exposure from neutrons having higher energies must be determined.

Some of these applications include working near spontaneous fission neutron sources, linear accelerators or cyclotrons, and in space flight.

The incident of a neutron beam upon a germanium detector produces atypical pulse height peaks whose shape changes with changes in the neutron energy. These peaks are asymmetrically broadened, with a sharp leading edge and a long high-energy tail.[4] The shape can be attributed to a combination of a prompt gamma ray or a combination electron line with the recoil energy of the germanium nucleus being transferred to electron-hole pairs. These peaks occur at 563, 596, 690, 835, 1035 keV. It has also been shown that as the energy of the incident neutron increases the broadening of these lines increase [4,5] however a search of the literature has indicated that there has been no determination of

the relationship of the broadening to the energy of the neutrons. It is the purpose of this paper to describe our results in evaluating the characteristics of these curves at various neutron energies.

A recent work [6] has described a method utilizing the 596 and 691 keV lines to estimate the dose rates of low flux neutrons. The neutron energy used for this analysis however did not exceed 2 MeV. An application of equations developed by Lindhard et al [7] show that kinematically at neutron energies above 4.5 MeV a portion of the 596 keV peak will merge into the 690 keV peak thus effectively reducing the total measured activity within this peak for their measurement. This will also occur at 6.6 MeV for the 690 keV peak merging into the 835 keV peak. The characteristics that we will use for evaluating these peaks will take this into account.

2. Data Setup

The 79 inch cyclotron at the Crocker Nuclear Laboratory on the campus of the University of California, Davis, was utilized to generate beams of energetic neutrons. Protons accelerated to energies of 20.5, 40.0 and 67.5 MeV were directed onto a 93 mil thick ^{7}Li target, with the $^{7}Li(p,n)^{8}Be$ reaction producing neutron beams with maximum energies of 18.8, 38.4 and 65.5 MeV. An Ortec GMX Series, Gamma-X HPGE, 5.0 cm diameter by 6.0 cm long, closed-end

high purity germanium detector was placed in the neutron beam for the 18.8 and 38.4 MeV runs. An Ortec GEM series HPGe, 5.1 cm diameter by 5.4 cm long coaxial high purity germanium detector was used for the 65.5 MeV run. Energy calibrations were performed with the 662 keV gamma rays of ^{137}Cs and the 1.17 and 1.32 MeV gamma rays of ^{60}Co. The 1.32 MeV gamma ray line was also utilized to check the energy resolution of the detector during the data acquisition. Germanium detectors are subject to damage from neutrons, [8] however, minimal changes in the energy resolution, measured before and after data acquisition, were observed in either detector.

Neutron doses to the detectors were estimated by the method described by Stelson et al. [8] to be 4.15×10^5 neutrons/cm^2 at 18.8 MeV, 1.38×10^6 neutrons/cm^2 at 38.4 MeV and 6.68×10^5 neutrons/cm^2 at 65.5 MeV.

Off-beam spectra were acquired during the 65.5 MeV neutron run to estimate the scattered neutron contribution to the spectra. This contribution to the spectra was estimated to be less than a few percent of the total data and not considered significant.

The spectra were acquired onto a personal computer utilizing the Nuclear Data Accuspeck acquisition and processing program. The data was stored to disc in the spectral and ASCII format. Figure 1 shows the spectra obtained during the 38.4 MeV neutron run displayed with the Canberra

System 100 spectral display system. The lower curve is the entire 4096 channel spectrum with the upper curve showing the areas of the spectrum with the recoil-broadened peaks. The 563, 596, 690, 835 keV lines were present at all three neutron energies. The 1035 keV line was seen in the spectra from the 18.8 and 38.4 MeV neutrons. The difficulty in defining the 1035 line from the 65.5 MeV neutrons was attributed to the low count rate obtained during this run. The 563 and 1035 keV lines were not considered for processing due to the low counting statistics.

3. Data Analysis

The ASCII coded data for all three neutron energies were transferred to the spectra analyzing program Ganymed [9]. This program uses a modified Gauss-Newton algorithm to fit the peaks with a polynomial background of order 1-6. A region of interest may be selected with a maximum of 150 channels. For the processing of the spectra used in this study, the area of interest was set to two channels prior to the upslope of the peak and extended to the first point of the upslope for the next peak. This end point was valid for the 596 and 690 keV peaks. For the 835 keV peak the full 150 channel limit was used to define the region of interest with the starting point the same as described above.

Three variables were entered affecting the fitting of the gamma ray peak and the shape of the background curve.

The first value P sets the degree of polynomial for the background curve fit. Values between one and six were allowable for this parameter. A higher value for the background polynomial allowed for a better fit to backgrounds of the type of curve expected from the recoil germanium atoms. A value of 5 or 6 was used for P throughout all data processing. The second variable sets the value of a residuum. The residuum was defined as the difference between each data point in the region of interest and the fitted value for that data point, divided by the standard deviation of the data point. The residuum acts as a sensitivity threshold for determining peaks; higher values reject more spurious peaks. For this work the highest residuum was used that allowed for the fitting of the primary gamma ray or electron conversion peaks for each selected peak. The third variable was the percent error rejection or confidence limit of the peak area. This value allows for the removal of peaks from the selection process if the confidence limit for the peak area exceeds this value. The higher this value was set the more likely a peak would be kept whether it was a spurious peak or a real peak. The default value of 30% was used for the processing of most peak selections. A 50% value was used for the 690 keV peak from the 65.5 MeV neutron run. This peak was difficult to fit due to low counting statistics and the 50% error provided for the selection and fitting of the 690 keV gamma ray peak.

After processing, the program presented a display of the raw data curve, the fitted curve and the background curve for the entered parameters. This background curve represents the portion of the curve resulting from the recoil germanium nucleus. The resultant curves for the 596 keV peak from the 18.8 MeV neutrons is shown in Figure 2.

Additional gamma ray photopeaks were present within the regions of interest used for the recoil peaks. These included the 609 keV peak which results from the transition of the 1205 keV excitation state of ^{74}Ge to 596 keV, and is also a gamma ray produced in the neutron capture and decay of ^{73}Ge. Also identified was the 846 keV peak resulting from the $^{27}Al(n,p)^{27}Mg$ reaction.

Three characteristics of the germanium recoil background curve were evaluated: 1) the full width at half, third, fourth, fifth, tenth and twentieth maximums; 2) the slope of different segments of the low energy upslope leg of the curve; and 3) the slope of the first leg of the high energy downslope segment of the curve.

The background germanium recoil portion of the printout was imported into the Lotus 123 program for evaluation of the full width measurements. Utilizing a macro for the Lotus program, full widths at half, third, fourth, fifth, tenth and twentieth maximum were calculated for each of the nine recoil curves. The results from this analysis are

presented in Table 2.

The next step was to evaluate the slopes of the recoil germanium spectra. The data was entered into another Lotus program called Graphwriter. This program has the capabilities of performing a group of regression fitting calculations for the entered data. The results are presented with a slope and intercept for the fit and a regression coefficient (R^2). An R^2 value of 1 indicates a perfect fit to the data. The slope measurements for these curves are the change in counts divided by the change in keV. The neutron energy curves all had approximately the same change in keV channel; however, the relative change in counts was vastly different. To overcome this relative difference in counts, all curves were normalized to a maximum count of 10000 for evaluation.

The upslope was evaluated with a linear fit over the first three, five and ten keVs of the curve. The slopes and the regression coefficients were recorded (see Table 3).

The first leg of the downslope was also evaluated with a linear fit. Four methods were used for selecting the area to be fitted. The first method was to select visually the most linear segments of the downslope leg. The other methods were based on determining the point on the downslope leg of the curve where the second derivative was equal to zero (zero point). This point was used as the center point for the area to be fitted. The second and third method utilized

the zero point and one and five points on either side of it, respectively. The fourth method utilized the maximum equal number of points on either side of the zero point that maintained a regression coefficient greater than 0.999. The absolute value of the slope was used to facilitate the use of the computer programs. Values are recorded in Table 4.

Figures 3 is a graphic representations of the upslope fitting utilizing the first five keV and the downslope fitting utilizing the second derivative zero point and ± 5 keV technique for point selection upon the 596 keV background curve of the 18.8 MeV run.

4. Discussion

The three different peaks (595, 690, 835 keV) that were evaluated were created in the same manner, i.e. the combination of gamma ray or electron conversion energy and the recoil germanium nucleus energy. The primary difference between the peaks should be the amount of energy the germanium nucleus transferred to the electron-hole pairs. It would therefore be reasonable to conclude that the three parameters evaluated would respond in a similar manner for all three recoil curves. However, when the full width measurements in Table 1 were graphed (Figures 4-6), the curves demonstrated that each of the peaks responded in a different manner as the energy of the neutrons increased.

It has been shown [4,5] that the curves were visually

wider with increasing neutron energy. However, the width calculations for the 596 keV peak decreased between neutron energies of 38.4 and 65.5 MeV and the 835 keV peak decreased over all three neutron energies. The 690 keV peak increased between each of the neutron energies, however, the amount it increased between 38.4 and 65.5 MeV was minimal. Figure 7 shows the normalized data for the 690 keV peak overlaid each other. This figure demonstrated that the amount of activity for the leading minimum point of each curve is greater at higher neutron energies.

The increase in the leading minimum point was caused by a "bleeding" of activity from the lower energy recoil curve into the curve of interest. The increase in the leading point value resulted in a higher calculated value of the width line and thus a smaller width measurement.

The kinematics of neutron scattering can explain the "bleeding" of activity from one curve into another. The maximum recoil energies were 984, 2024 and 3504 keV for the 18.8, 38.4 and 65.5 MeV neutrons respectively at a Q value of -0.596 MeV. For a Q value of -0.690 MeV the maximum recoil energies were 1010, 2080 and 3580 keV.

The energy transferred to the electron-hole pairs from the recoil germanium nuclei, as calculated with Lindhard's equations [7] is shown in Figures 8 and 9. There is a 33 keV difference between the 563 and 596 keV recoil energy levels. The difference between 596 and 690 keV is 94 keV and

between 690 and 835 keV is 140 keV. The results shown in Figures 8 and 9 indicate that much of the recoil energy from the lower excitation state was recorded in the higher excitation levels. As the neutron energy increased, the maximum amount of energy that was transferred to the electron-hole pairs also increased and more of this activity appeared in the next higher excitation state. Figure 10 schematically demonstrates this relationship between the two excitation state.

It was seen from the data shown in Table 3 the upslopes measured at 3, 5 or 10 keV all followed a similar pattern. When this data was graphed, with the neutron energy on the x-axis and the slope plotted on a logarithmic scale, all three recoil peaks plotted a straight line. The graphs for the 5 keV slope fittings are shown in Figure 11.

A logarithmic fit was performed on each of these lines to determine an equation to describe the lines in the form:

$$Y = a(e^{(bX)}) \qquad 1$$

where a is the intercept and b is the slope of the line. All three recoil peaks presented the same pattern (Figure 12).

In following the argument that an increase in neutron energy will result in a larger "bleeding" from a lower to a higher peak, it was noted that the curves from the 65.5 Mev neutrons demonstrated a spread of only 13 keV from the initial point of the curve to the maximum point. Consequent-

ly, if this determination were to extend beyond the neutron energies studied, the 10 keV slope determination would begin to involve portions of the peak and downslope and no longer be a true measure of the upslope. Tables 4 and 5 present values for a, b and the R^2 regression coefficient for the 3 and 5 keV fits respectively.

Solving equation 1 for X, the neutron energy and using a factor to account for the normalization of the recoil curves to a maximum count of 10000 results in the equation:

$$X = (\ln (S * (10000/M))/a)/b. \qquad 2$$

where X = Neutron energy
S = Slope of first 3 or 5 keV of upslope for the recoil curve
M = Maximum count in recoil curve
a and b are values for the respective curves found in Tables 5 and 6.

The downslope values from Table 3 were plotted on a log-log scale (see Figure 13 for the 11 keV values). These values when plotted demonstrated a straight line. However, a mild variation was observed for the 835 keV recoil curve. There was excellent agreement among the four methods used for determining the slope of the curves.

The 835 keV curve probably has reached a point where a large change in neutron energy was needed to show a small change in the downslope of the recoil curve. An evaluation of this curve should be performed at energies between 18.8 and 38.4 MeV to determine where this transition occurred.

The 596 and 690 keV recoil curves were fitted with a

power function:

$$Y = aX^b \qquad 3$$

a and b again represent the intercept and slope of these fitted lines, respectively (Figure 14). Both the visual and maximum ($R^2 > 0.999$) determinations required multiple guesses as to the end points of the fitted areas. This would result in an excessive amount of time for the users of this type of evaluation. Although the results from the visual and maximum types of selections were very similar to the results obtained for the 3 and 11 keV lines the latter two will be discussed here. Tables 6 and 7 present the values for a, b and R^2 for these fittings.

Using the same symbol designation used for the upslope equation and solving equation 5.10 for the neutron energy yields:

$$X = (-S * (10000/M)/a)^{(1/b)} \qquad 4$$

The negative sign appears before the slope value S to account for the negative downslope. The downslopes were plotted as an absolute value in order to perform the power fitting on the computer.

Both line lengths provided a reasonable estimation of the maximum neutron energy used to produce the slopes. There appeared to be very little difference between the 3 and 11 keV line lengths used for the slope measurements. The maximum spread and visual selections had similar results.

5. Conclusion

The recoil germanium portion of a spectrum produced by the (n, n'γ) inelastic scattering of the neutron and the germanium nucleus was used to evaluate the maximum energy of the neutron beam. It was shown that the full width measurements of the curve do not provide an accurate measurement of the neutron energy. The upslope and the first leg of the downslope of these curves provided a group of equations that provided a reasonable estimate of the maximum energy of the neutron beam. The following group of equations were derived:

596 KEV CURVE

Upslope Equations:

3 keV Fit $X = (\ln ((S \times (10000/M))/369.10142))/-0.009220$

5 keV Fit $X = (\ln ((S \times (10000/M))/367.80462))/-0.010744$

Downslope Equations:

3 keV Fit $X = ((-S \times (10000/M))/508.31277)^{-1.67256}$

11 keV Fit $X = ((-S \times (10000/M))/495.78060)^{-1.68253}$

690 KEV CURVE

Upslope Equations:

3 keV Fit $X = (\ln ((S \times (10000/M))/788.05459))/-0.025537$

5 keV Fit $X = (\ln ((S \times (10000/M))/695.88448))/-0.024935$

690 KEV CURVE

Downslope Equations:

3 keV Fit $X = ((-S \times (10000/M))/1417.5361)^{-1.21022}$

11 keV Fit $X = ((-S \times (10000/M))/1345.4889)^{-1.22762}$

835 KEV CURVE

Upslope Equation:

3 keV Fit $X = (\ln ((S \times (10000/M))/359.44913))/-0.018135$

5 keV Fit $X = (\ln ((S \times (10000/M))/343.28974))/-0.019077$

It should be noted that these equations are only valid under low neutron flux conditions. Care should be taken to ensure that the dead time of the detector is low.

For quasi-monoenergetic neutron beams the high-purity coaxial and planar germanium detectors were found to be useful instruments in determining the maximum neutron energy. It is reasonable to conclude that these results will also apply to accelerator produced (structured) white-neutron sources; however, the application to spectra produced by continuous energy neutron(non-structured) sources would not be valid. The germanium detector can be used to not only measure gamma ray spectra by the Health Physicist but also as a useful tool in estimating the dose rate from a neutron source. To continue this evaluation, these equations should be verified with other neutron sources and their validity evaluated at higher neutron energies.

Table 1

Width Measurements (keV) for the Recoil Germanium Curves

	Curves (keV)								
	596			690			835		
	Neutron Energy (MeV)								
Peak Width	18.8	38.4	65.5	18.8	38.4	65.5	18.8	38.4	65.5
Half	42.5	48.0	33.4	26.3	30.9	33.9	69.1	53.1	29.2
Third	56.3	60.8	41.1	31.7	37.6	39.4	93.3	37.6	34.9
Fourth	67.7	69.8	45.5	34.5	41.4	42.9	102.7	81.3	36.9
Fifth	75.3	76.9	48.2	36.3	43.4	44.0	108.0	87.4	38.7
Tenth	85.8	89.9	54.1	40.3	51.3	48.6	119.7	98.4	42.5
20th	93.3	94.1	57.3	42.1	53.3	50.8	124.2	103.4	44.5

Table 2

Upslope Fittings and Regression Coefficient Values

Curve Peak keV	Neutron Energy MeV	3 keV	R^2	5 keV	R^2	10 keV	R^2
596							
	18.8	313.2	0.9999	302.9	0.9993	270.6	0.9962
	38.4	255.0	0.9998	240.2	0.9987	203.7	0.9922
	65.5	203.1	0.9988	183.0	0.9953	138.6	0.9759
690							
	18.8	474.2	0.9991	423.1	0.9950	310.3	0.9691
	38.4	310.1	0.9993	280.7	0.9962	213.9	0.9734
	65.5	145.0	0.9995	133.1	0.9973	106.9	0.9853
835							
	18.8	256.3	0.9997	239.5	0.9983	200.8	0.9911
	38.4	178.3	0.9995	165.4	0.9988	135.9	0.9889
	65.5	109.8	0.9991	98.3	0.9954	73.0	0.9723

Table 3

Absolute Value of Downslope Fittings
and Regression Coefficient Values

Curve Peak (kev) Neutron Energy (MeV)	Visual	R^2	3 Point*	11 Point	R^2	Maximum Points	R^2
596							
18.8	85.8	0.9998	88.9	87.5	0.99995	83.4	0.9992
38.4	53.6	0.9996	56.0	55.5	0.99998	52.6	0.9992
65.5	40.0	0.9991	42.3	41.8	0.99997	39.9	0.9991
690							
18.8	117.9	0.9994	123.1	120.8	0.99993	117.0	0.9992
38.4	69.8	0.9993	72.8	72.3	0.99996	68.8	0.9992
65.5	41.8	0.9994	43.6	43.4	0.99993	41.8	0.9991
835							
18.8	33.2	0.9992	35.3	34.6	0.99993	32.6	0.9990
38.4	27.3	0.9995	28.6	28.3	0.99999	26.9	0.9991
65.5	26.9	0.9992	28.4	28.1	0.99996	27.1	0.9993

* All R^2 are greater than 0.9999999

Table 4 Line Function Parameters for the 3 keV Upslope Fit

Peak Curve	b	a	R^2
596	-0.009220	369.10142	0.9960160
690	-0.025537	788.05459	0.9951706
835	-0.018135	359.44913	0.9999077

Table 5 Line Function Parameters for the 5 keV Upslope Fit

Peak Curve	b	a	R^2
596	-0.010744	367.80462	0.9978301
690	-0.024935	695.88448	0.9945830
835	-0.019077	343.28974	0.9999789

Table 6 Line Function Parameters for the 3 keV Downslope Fit

Recoil Curve	b	a	R^2
596	-0.597885	508.3128	0.9967462
690	-0.826296	1417.5361	0.9942136

Table 7 Line Function Parameters for the 11 keV Downslope Fit

Recoil Curve	b	a	R^2
596	-0.594343	495.7806	0.9974738
690	-0.814584	1345.4889	0.9933723

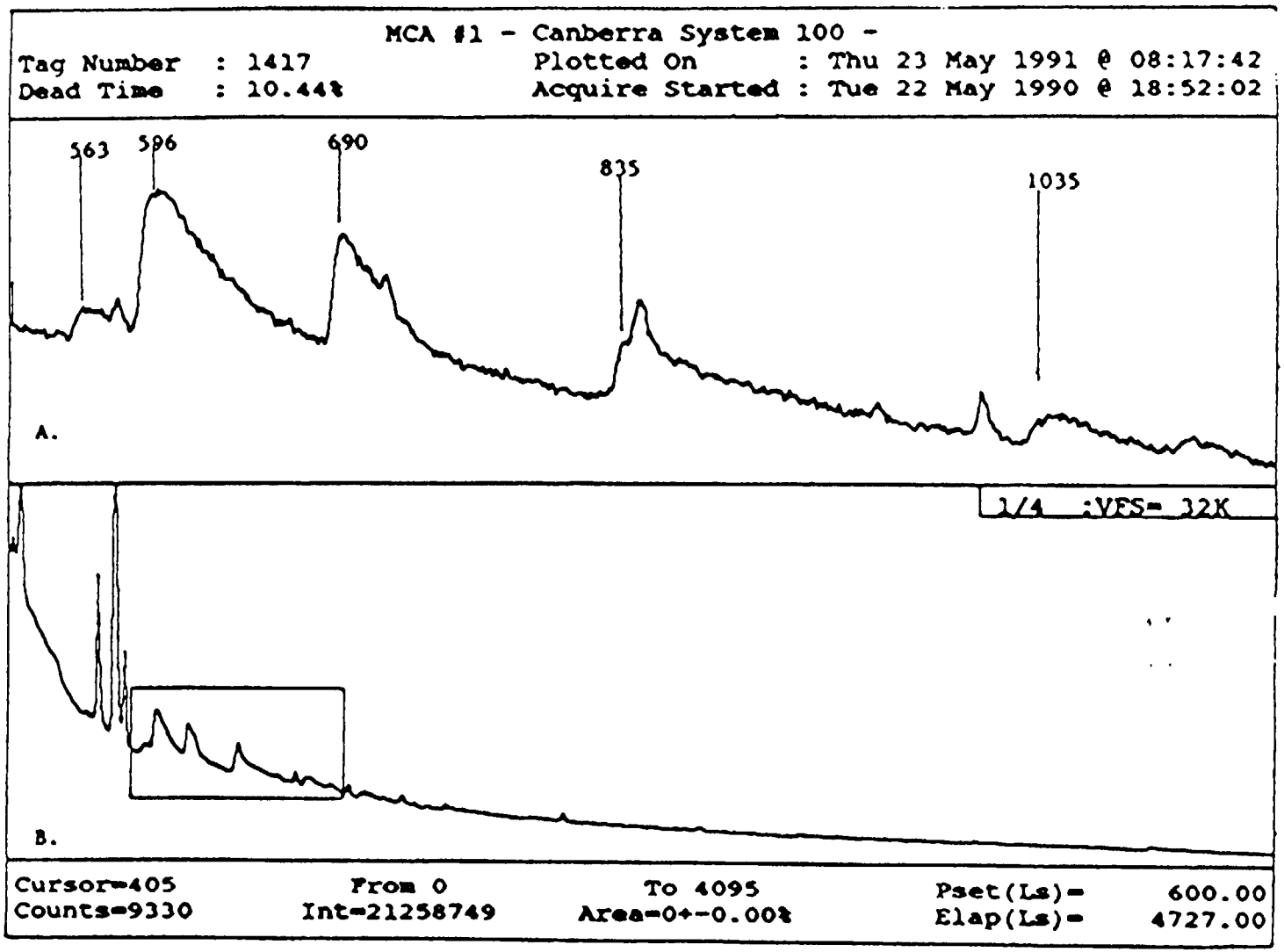

Fig 1 Acquired Spectrum for 38.4 MeV Neutrons A. Region of Recoil Curves
B. Full 4096 Channel Spectrum

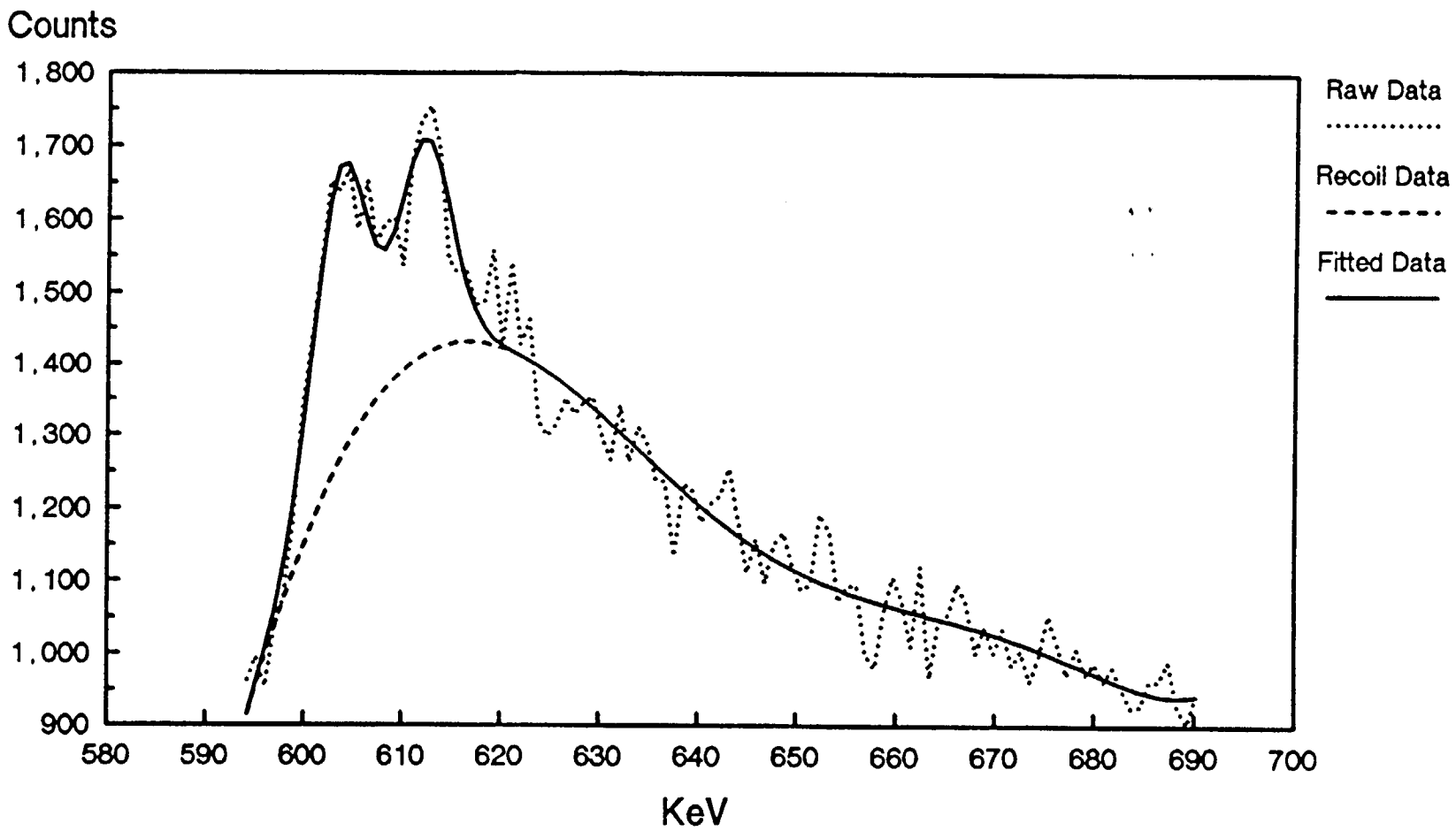

Fig. 2 Ganymed Fitting of 596 keV Peak from
18.8 Mev Neutrons

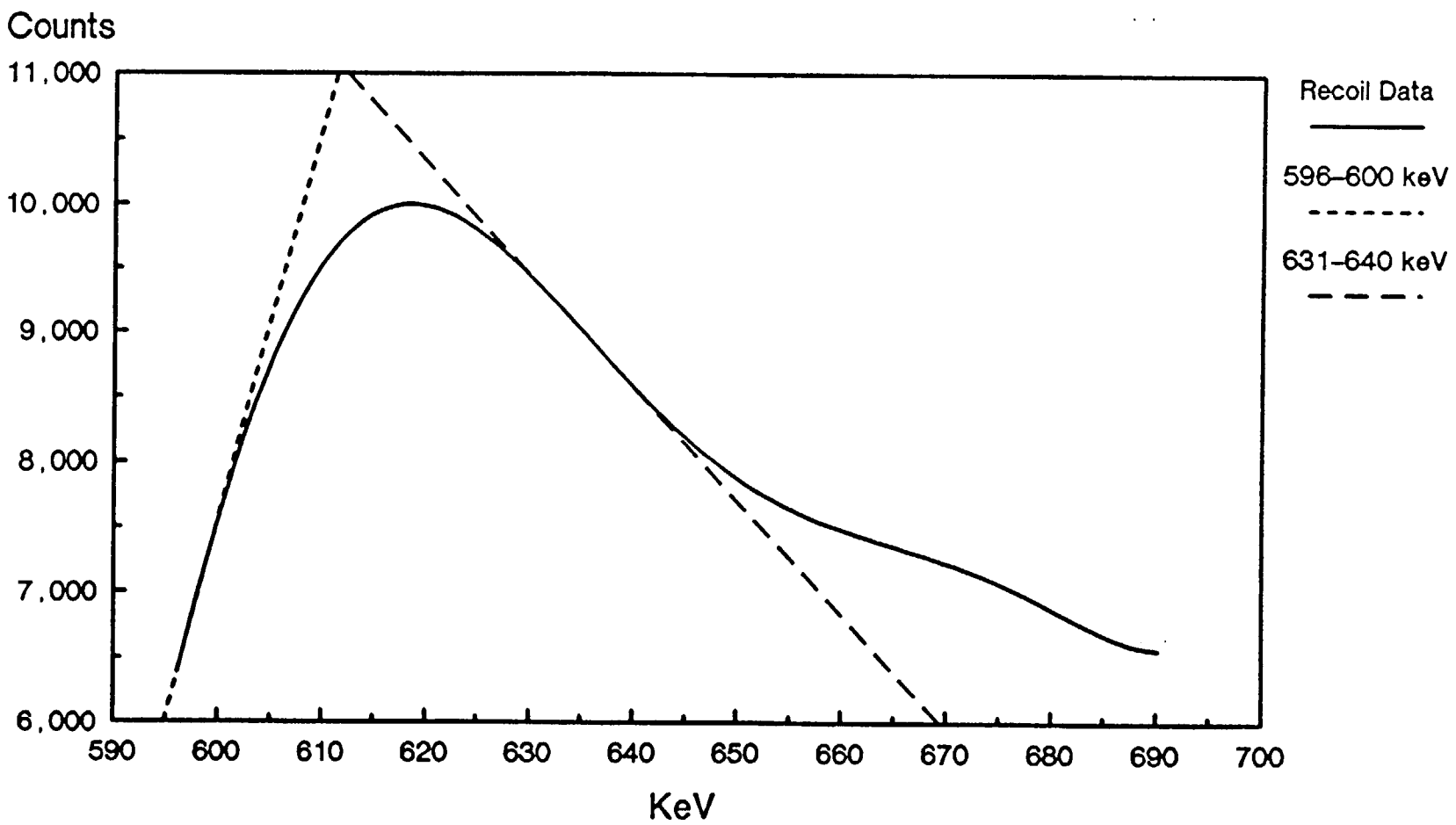

Fig. 3 Slope Fittings for 596 keV Recoil Data from 18.8 MeV Neutrons

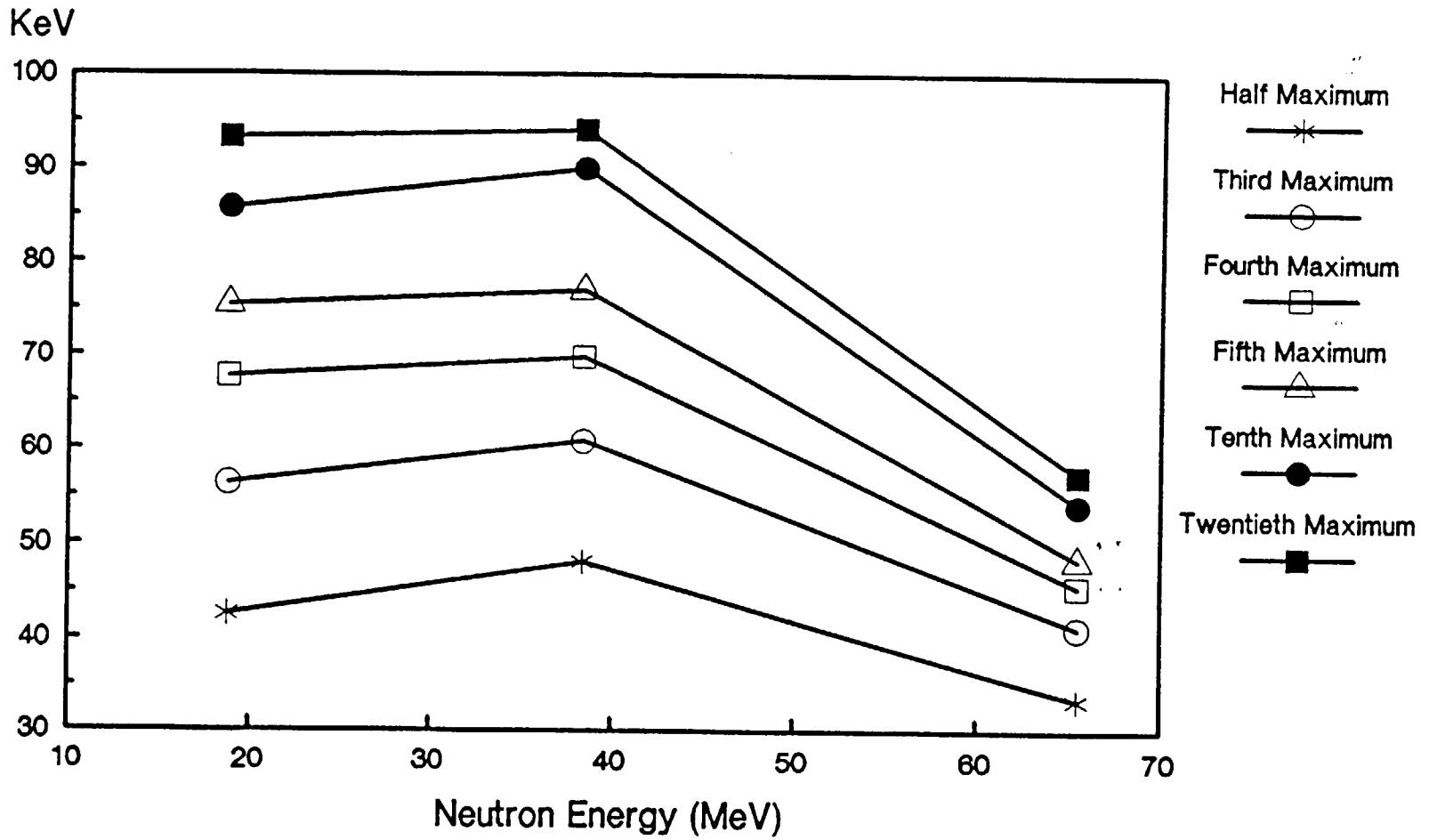

Fig. 4 Curve Width Comparisons for 596 keV Recoil Data

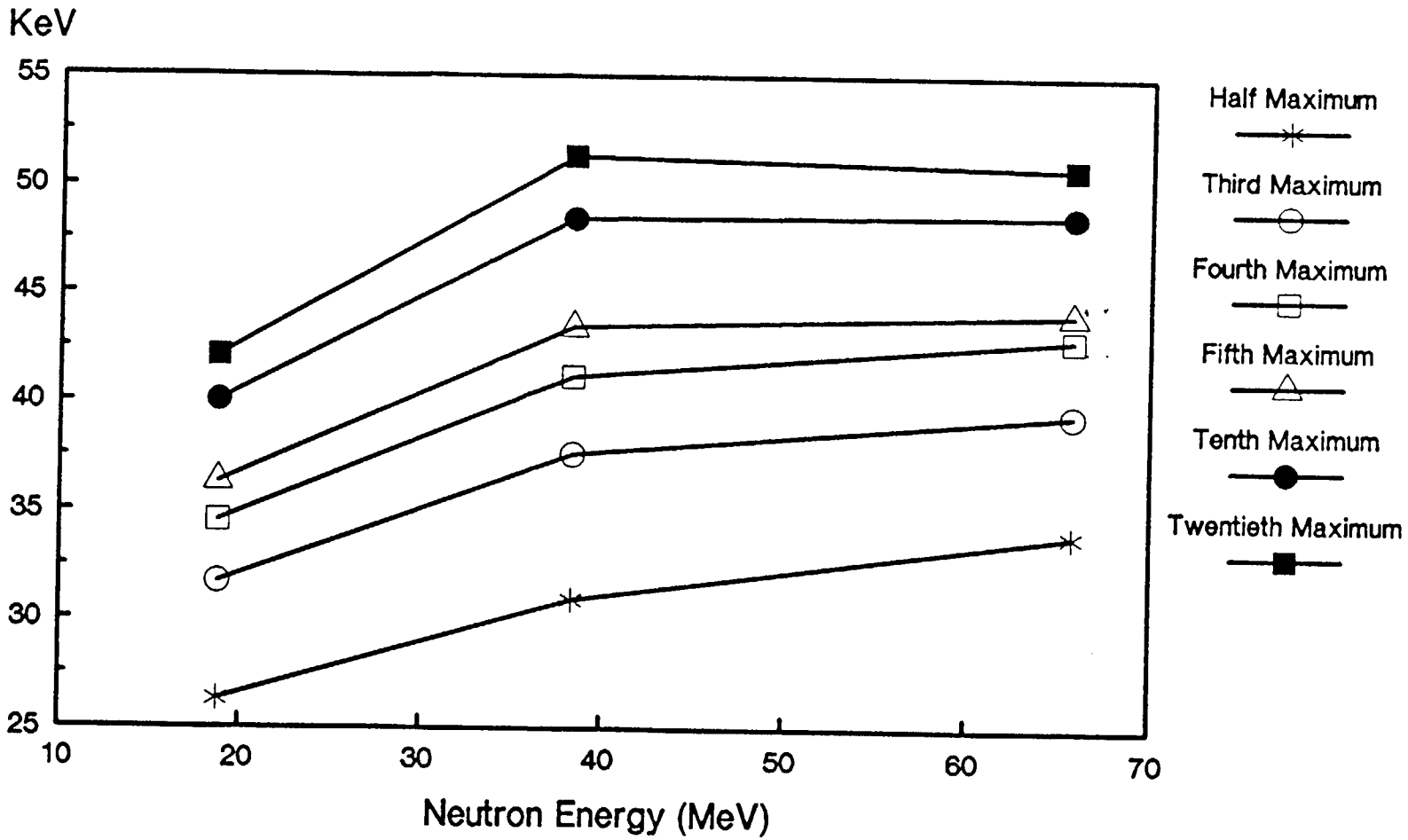

Fig. 5 Curve Width comparisons for 690 keV Recoil Data

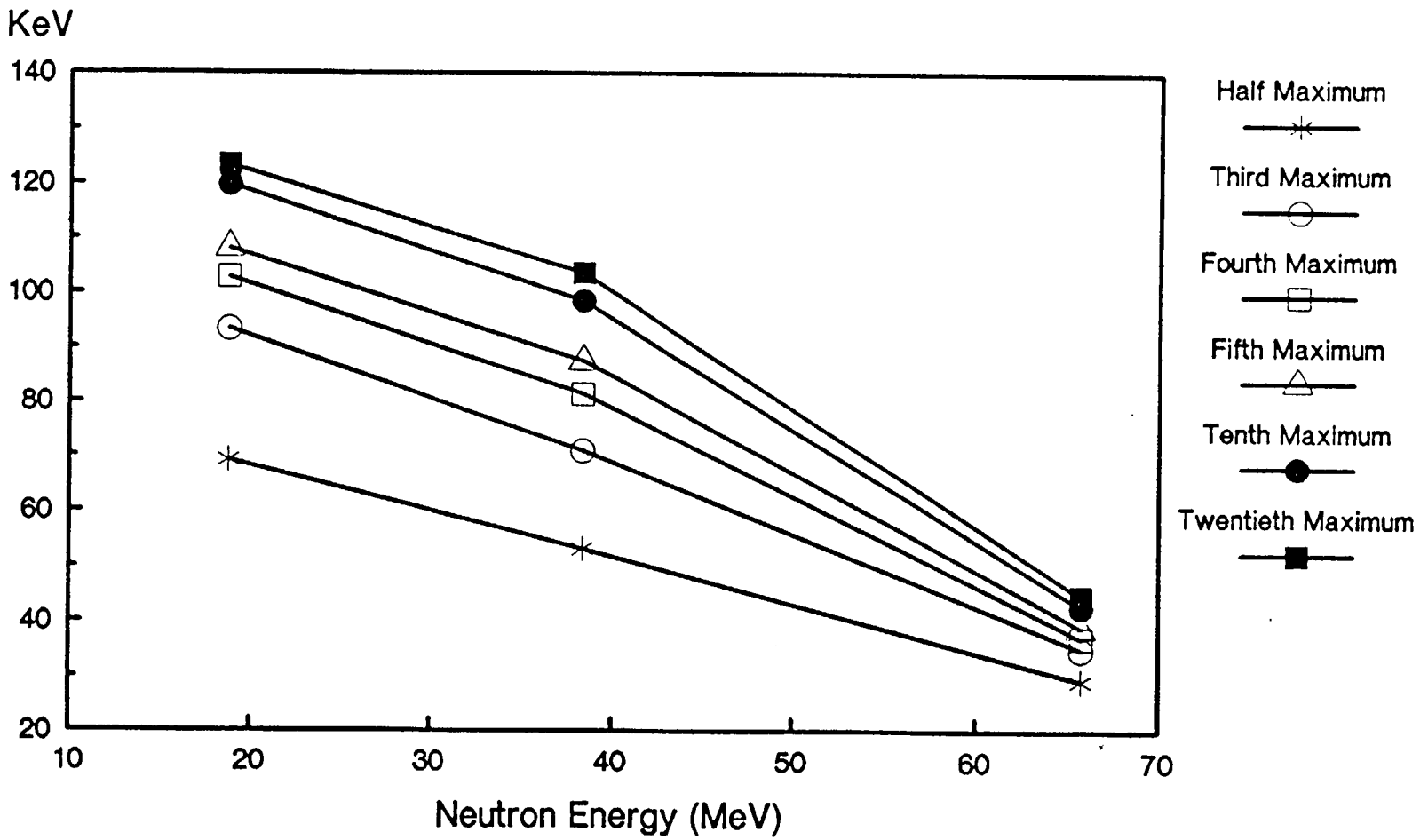

Fig. 6 Curve Width Comparison for 835 keV Recoil Data

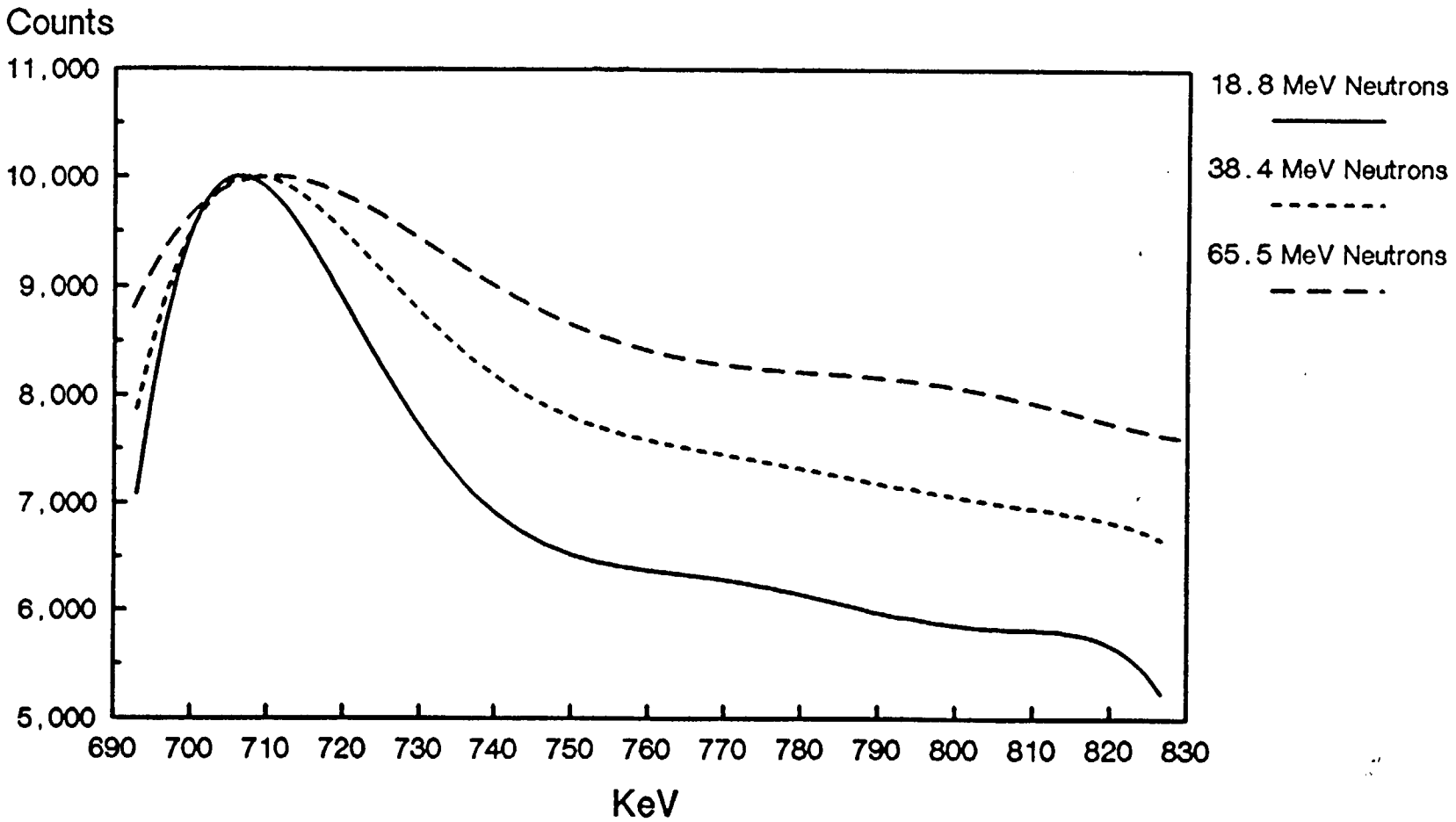

Fig. 7 Normalized Overlay of 690 keV Recoil Data

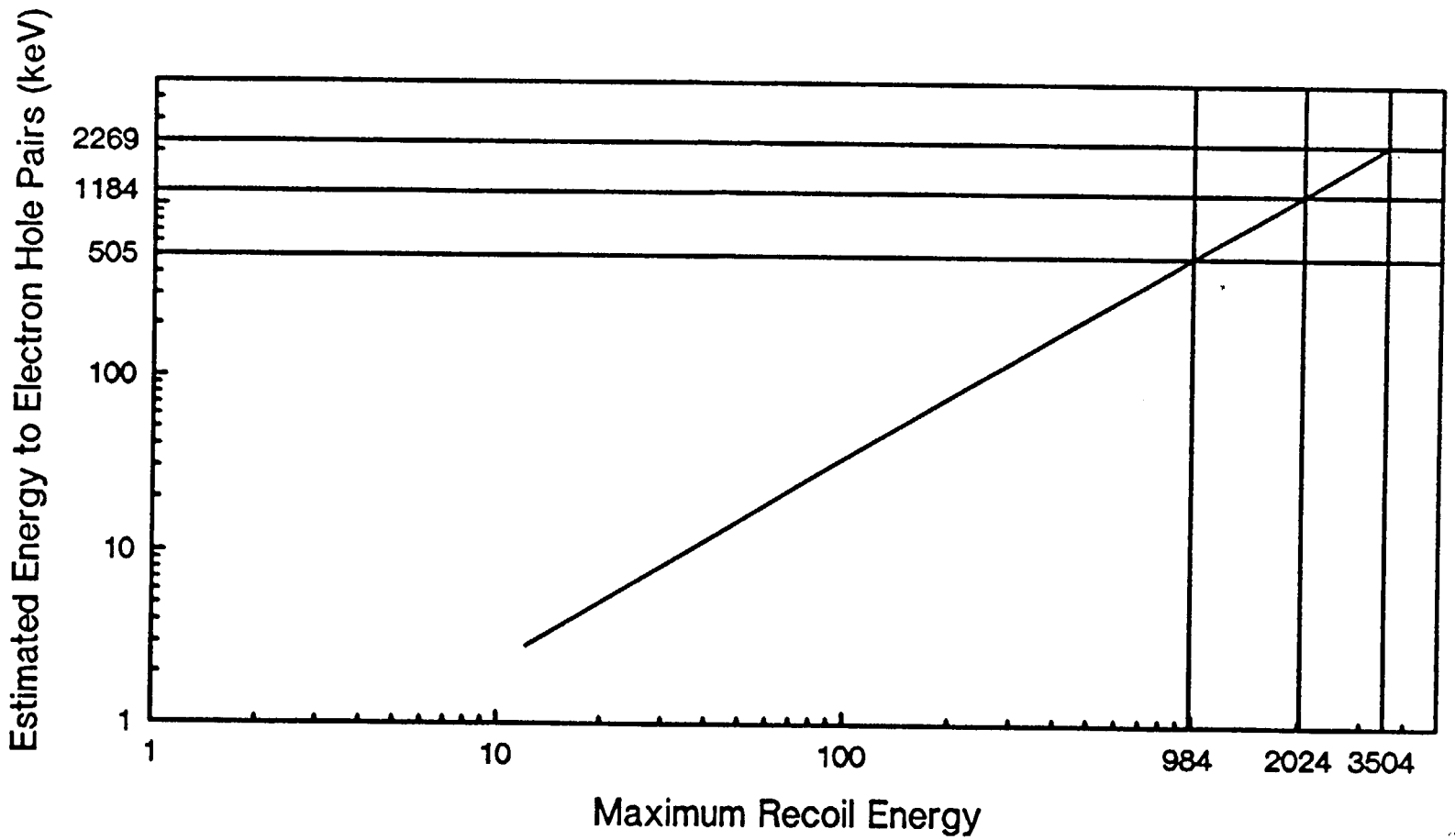

Fig. 8 Relationship between Recoil Energy and Energy Transfered to Electron Hole Pairs for 596 keV Recoil Data

Adapted From Lindhard et al.

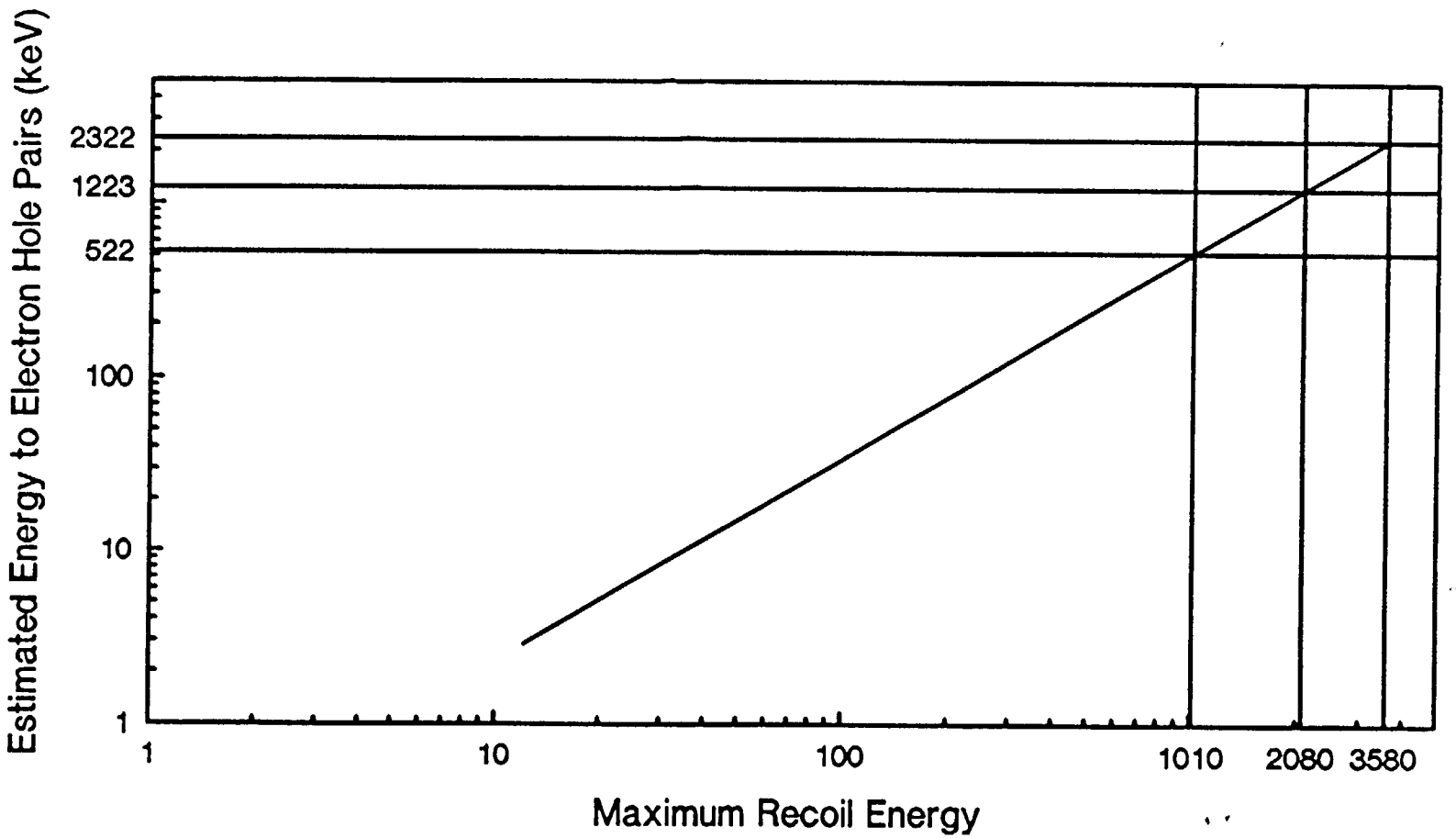

Fig. 9 Relationship between Recoil Energy and Energy Transfered to Electron Hole Pairs for 690 keV Recoil Data

Adapted From Lindhard et al.

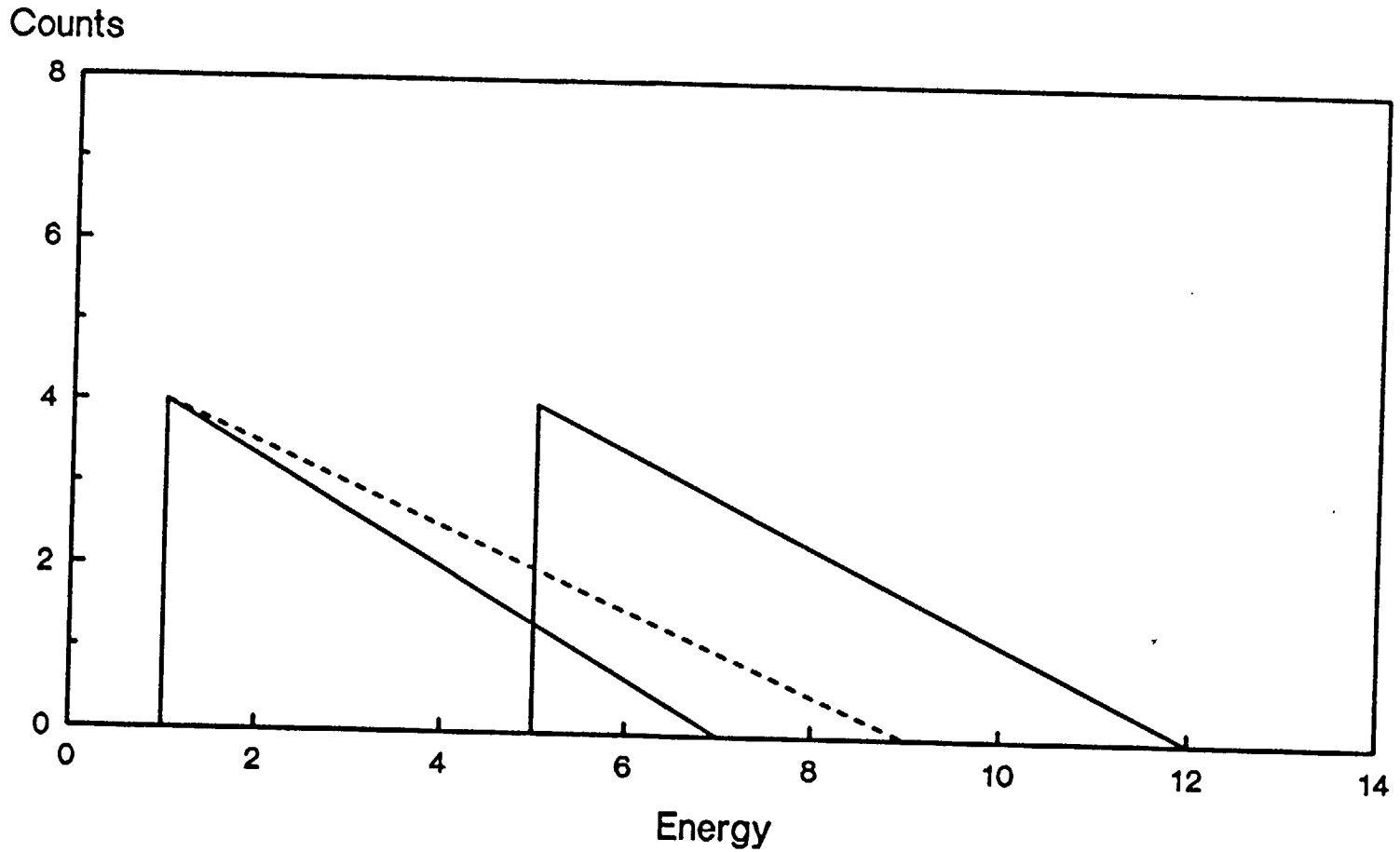

Fig. 10 Schematic Representation of the Bleeding of Recoil Energy from One Excitation State to the Next High Excitation State

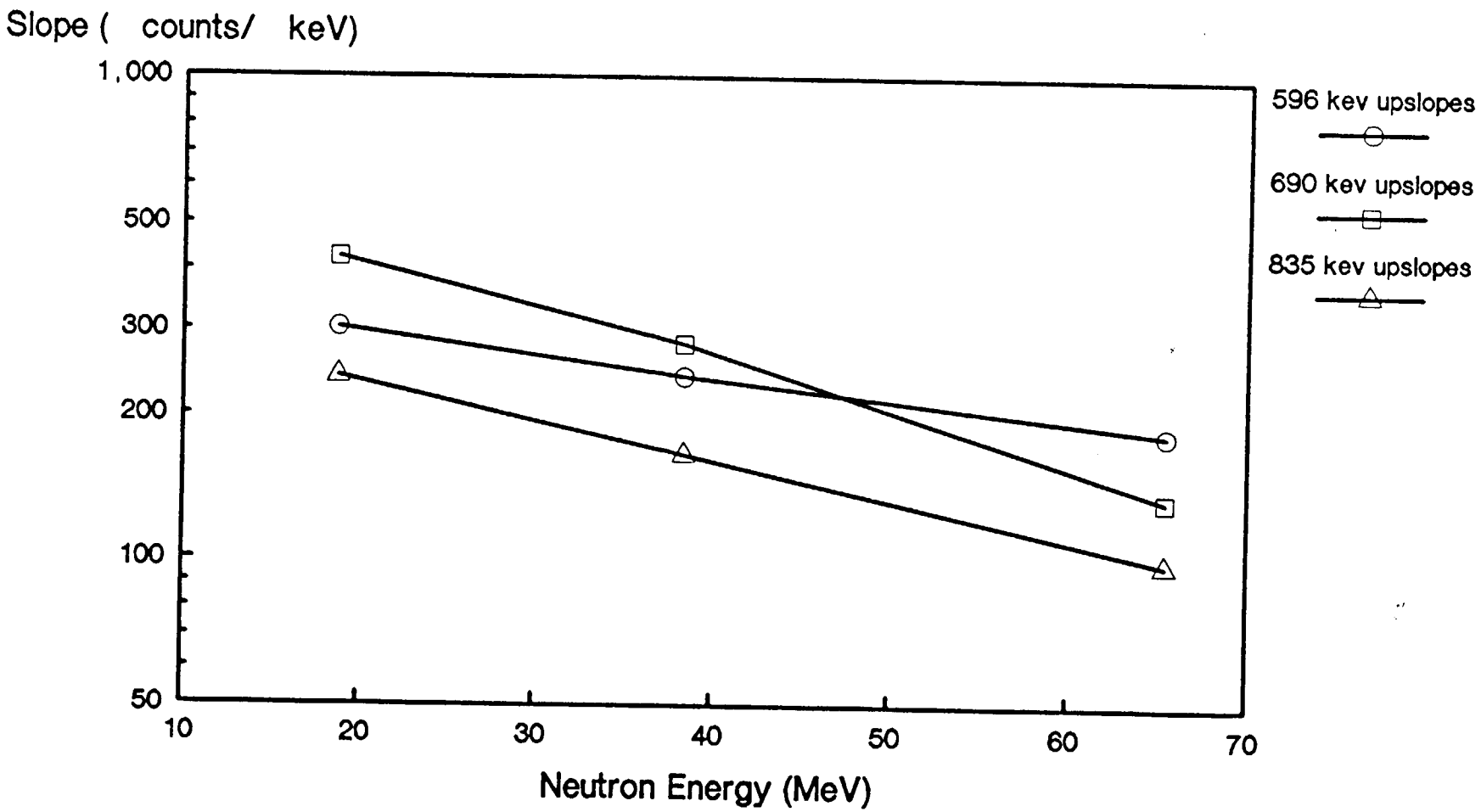

Fig. 11 Linear Slope Fittings for the Upslope Leg Determined from 5 keV Segments

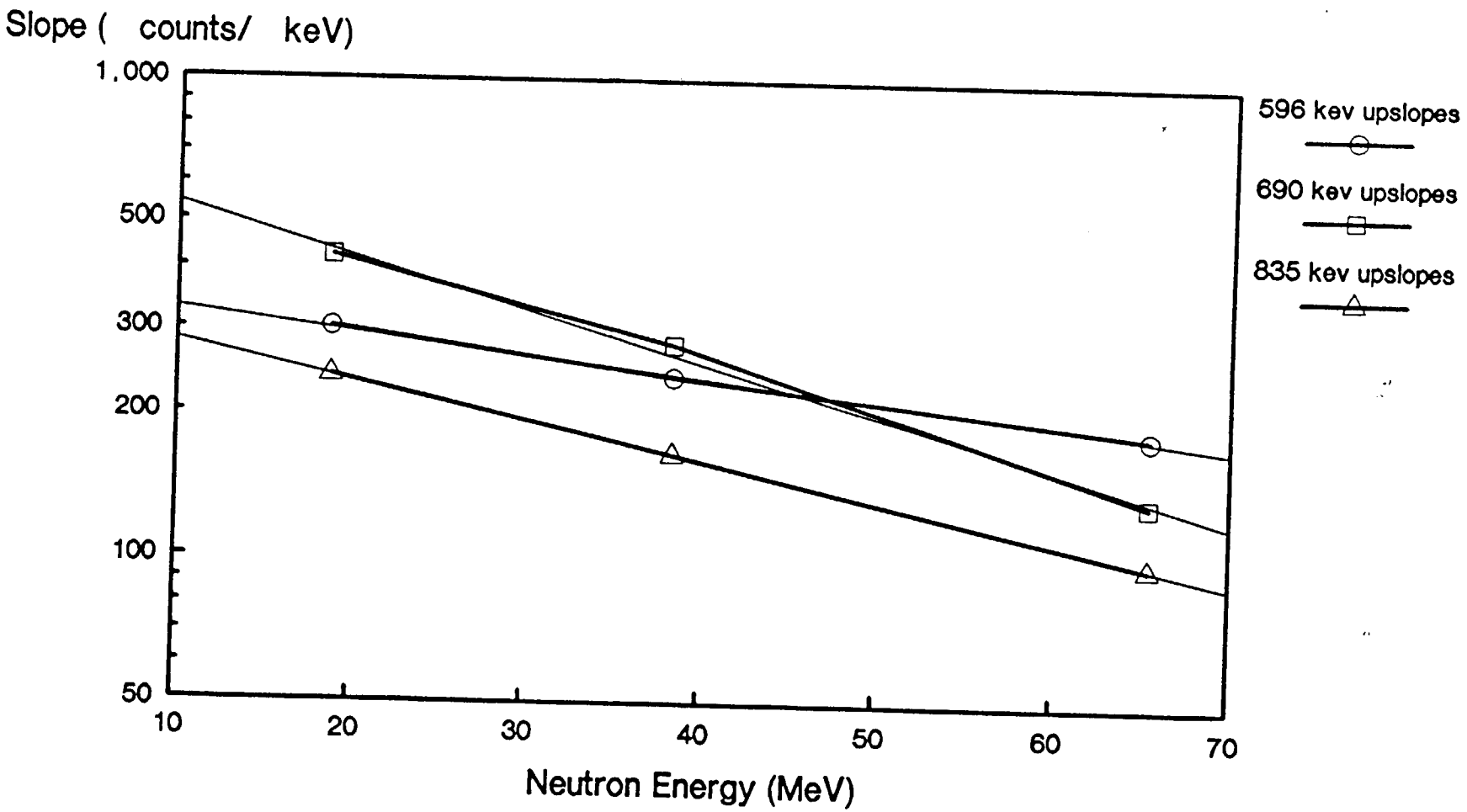

Fig. 12 Logarithmic Fitting of the Linear Upslope Values

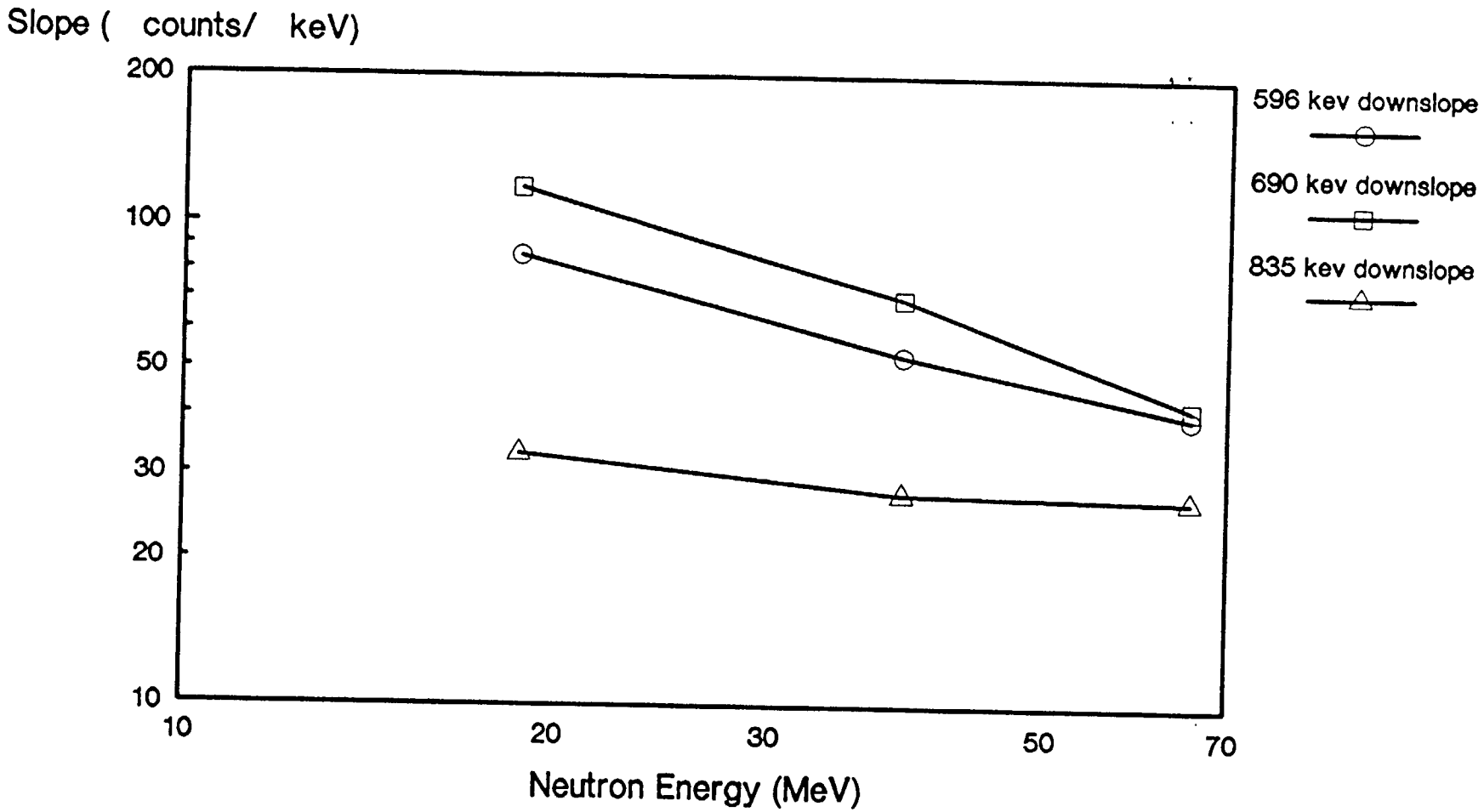

Fig. 13 Linear Slope Fitting for the Downslope Leg Determined From 11 keV Segments

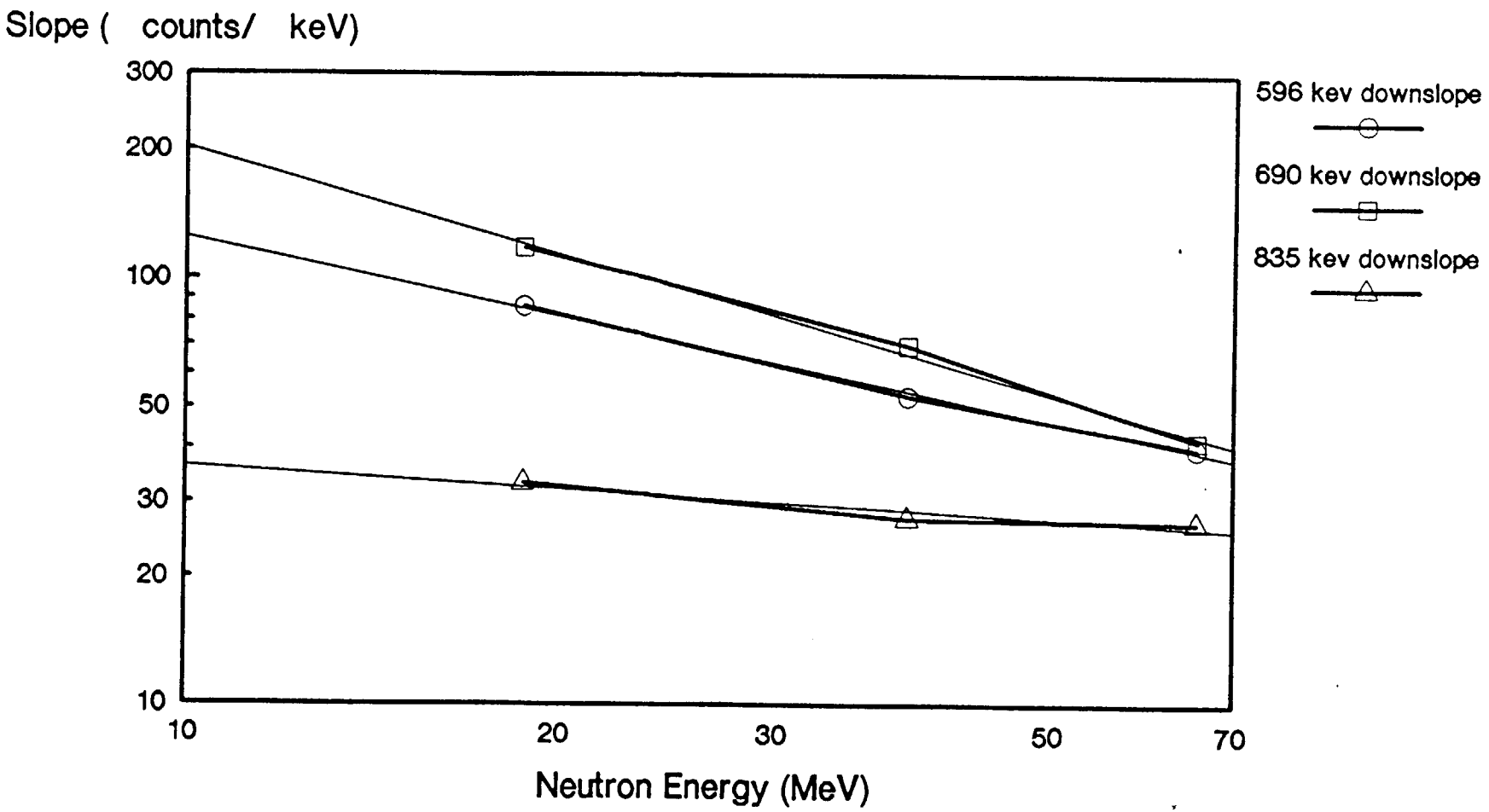

Fig. 14 Power fitting of the Linear Downslope Values

REFERENCES

[1] Attix, F. H. (1986). Introduction to Radiological Physics and Radiation Dosimetry. New York:John Wiley and Sons.

[2] Protection Against Neutron Radiation (1971) Report #38. Washington D.C.:National Council on Radiation Protection and Measurements.Cember, H., (1985) Introduction to Health Pysics (2nd ed.). New York:Pergamon.

[3] Cember, H., (1985) Introduction to Health Physcis (2nd ed.). New York:Pergamon.

[4] Chasman, C., Jones, K. W., Ristinen, R. A. (1965a). Fast neutron bombardment of a lithium-drifted germanium gamma-ray detector. Nuclear Instruments and Methods, 37, 1-8.

[5] Smith, D. L. (1972). Fast-neutron flux measurement with a Lithium-drifted germanium detector. Nuclear Instruments and Methods, 102, 193-199.

[6] Chung, C., Chen, R. C., (1991), Application of a germanium detector as a low flux neutron monitor. Nuclear Instruments and Methods in Physics Research, A301, 328-336.

[7] Lindhard, J., Nielsen, V., Scharff, M., Thomsen, P. V., (1963). Fys. Medd. Dan. Vid. Selsk, 33.

[8] Stelson, P. H., Dickens, J. K., Raman, S., Trammell, R. C. (1972). Deterioration of large Ge(Li) diodes caused by fast neutrons. Nuclear Instruments and Methods, 98, 481-484.

[9] Kruse, H., Spectra processing with computer-graphics, In Carpenter, B. S., D'Agostino, M. D., and Yule, H. P. (Eds) Computers in Activation Analysis and Gamma-Ray Spectroscopy, Department of Energy: Proceedings of American Nuclear Society Topical Conference. Mayaguez, Puerto Rico.